Radboud Universiteit Nijmegen

IMM Institute for Molecules and Materials

Graphene: CERN on the desk

Mikhail Katsnelson

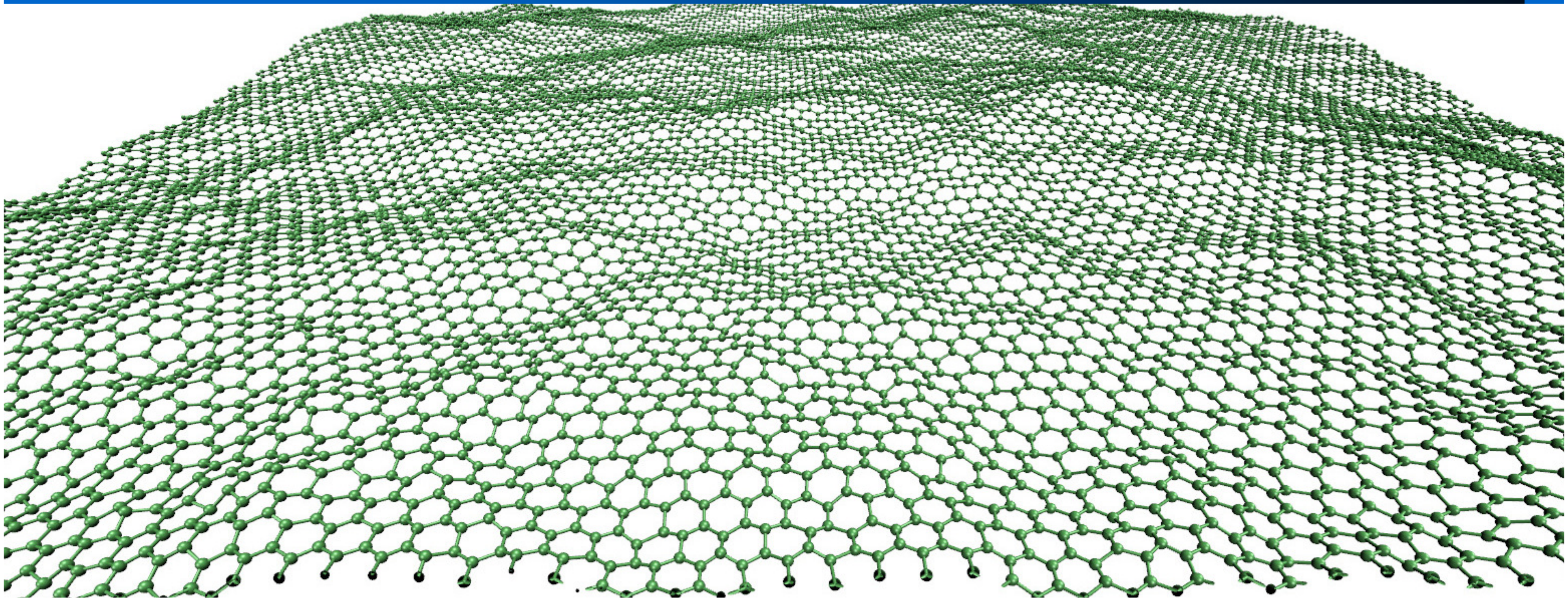

Instead of epigraph

You can get much further with a *kind word* and a *gun* than you can with a *kind word* alone
(Al Capone)

You can get much further with an insight from experiment and mathematics than you can with mathematics alone

Why graphene is interesting?

Till 2004: a way to understand graphite, nanotubes, fullerenes + theoretical interest (Dirac point Wallace 1947, McClure 1956…)

Do we theoreticians need experimentalists?! – Yes!!! (Klein tunneling, supercritical charge, ripples, new wave equation – bilayer, new type of transport…)

1. *Applications (modern electronics is 2D, bulk is ballast)*
2. *Prototype membrane (new drosophila for 2D statistical mechanics)*
3. *CERN on the desk (mimic high energy physics)*

Massless Dirac fermions

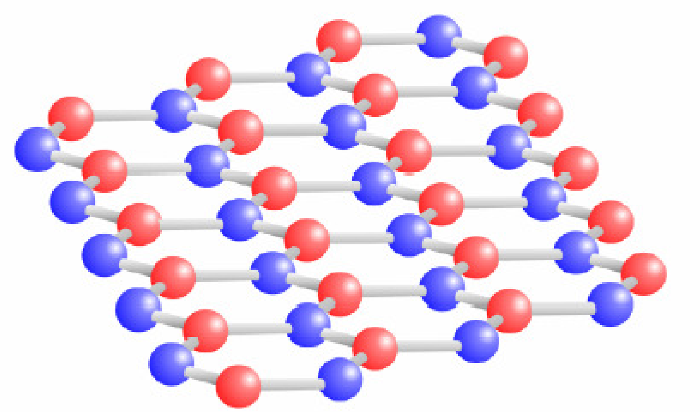

pseudospin

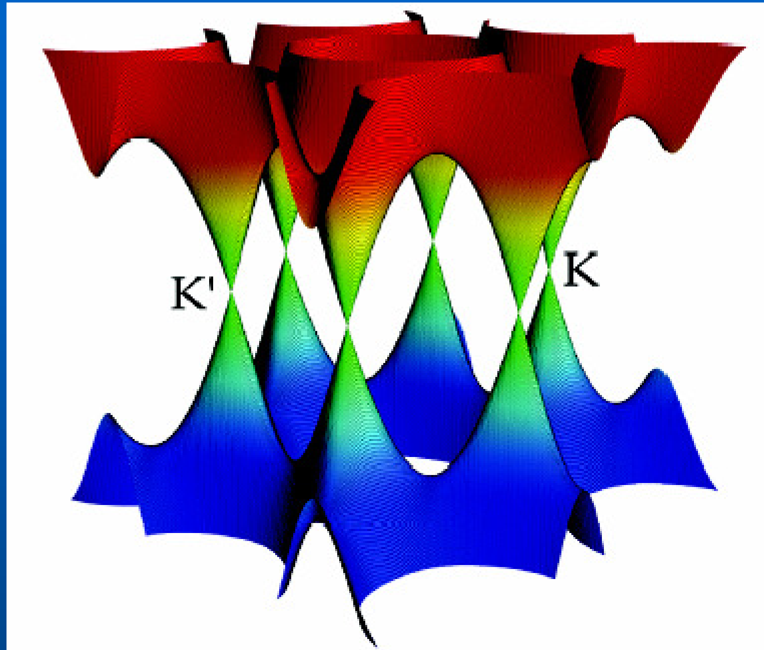

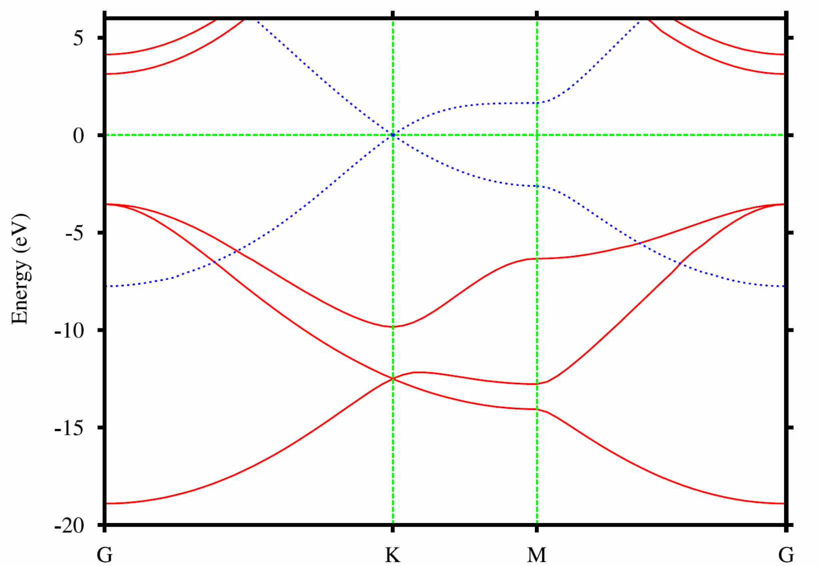

FIG. 2: (color online) Band structure of a single graphene layer. Solid red lines are σ bands and dotted blue lines are π bands.

sp^2 hybridization, π bands crossing the neutrality point

Neglecting intervalley scattering: massless Dirac fermions

Symmetry protected (T and I)

Outline

Minimal conductivity problem and transport via evanescent waves

Klein tunneling and inhomogeneities

Gauge pseudomagnetic fields and strain engineering

Relativistic collapse for supercritical charges

Quantum-Limited Resistivity

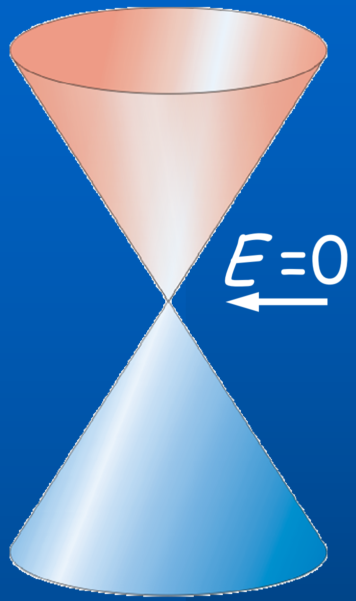

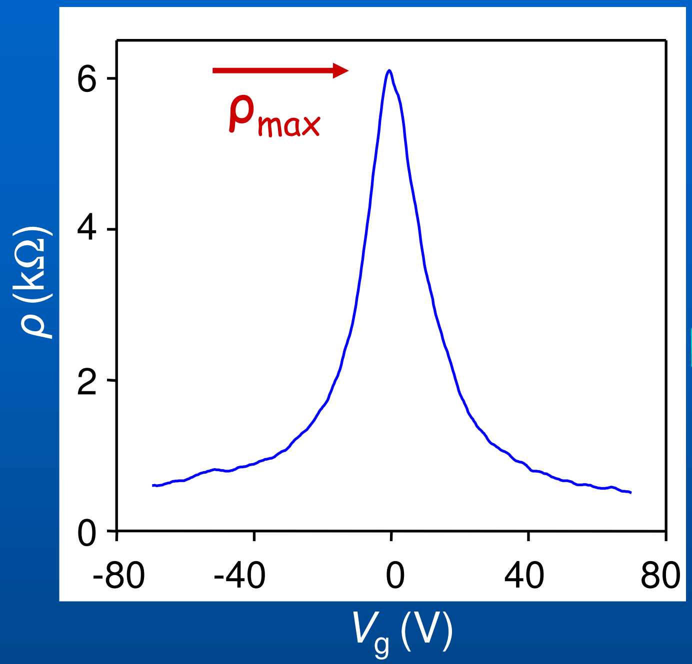

no temperature dependence in the peak between 3 and 80K

zero-gap semiconductor

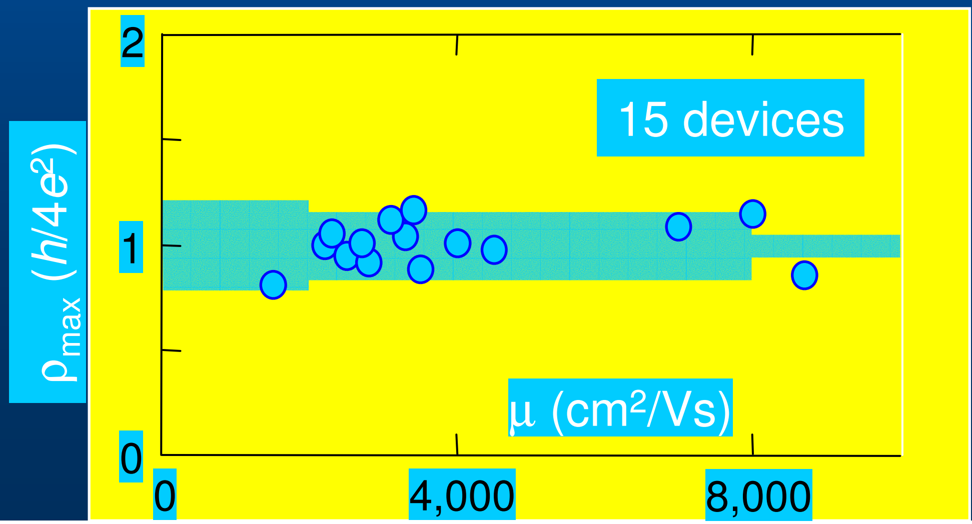

Novoselov et al, Nature 2005

Problem of minimal conductivity

At zero doping, zero temperature there is a finite minimal conductivity approximately e^2/h per channel

Two views: from the side of no disorder and from the side of strong disorder

Amazing property of 2D massless particles: finite conductivity for ideal crystal – no scattering, no current carriers! (Ludwig et al, PR B 1994)

Transport via evanescent waves

MIK, EPJ B 51, 157 (2006)

Conductance = $e^2/h\ Tr\ T$ per valley per spin

T is the transmission probability matrix

The wave functions of massless

Dirac fermions at zero energy:

$$\left(\frac{\partial}{\partial x} \pm i \frac{\partial}{\partial y}\right)\psi_{\pm}(x,y)=0 \qquad\qquad \psi_{\pm}(x,y)=f(x \pm iy) \qquad \forall f$$

Boundary conditions determine the functions *f*

Transport via evanescent waves II

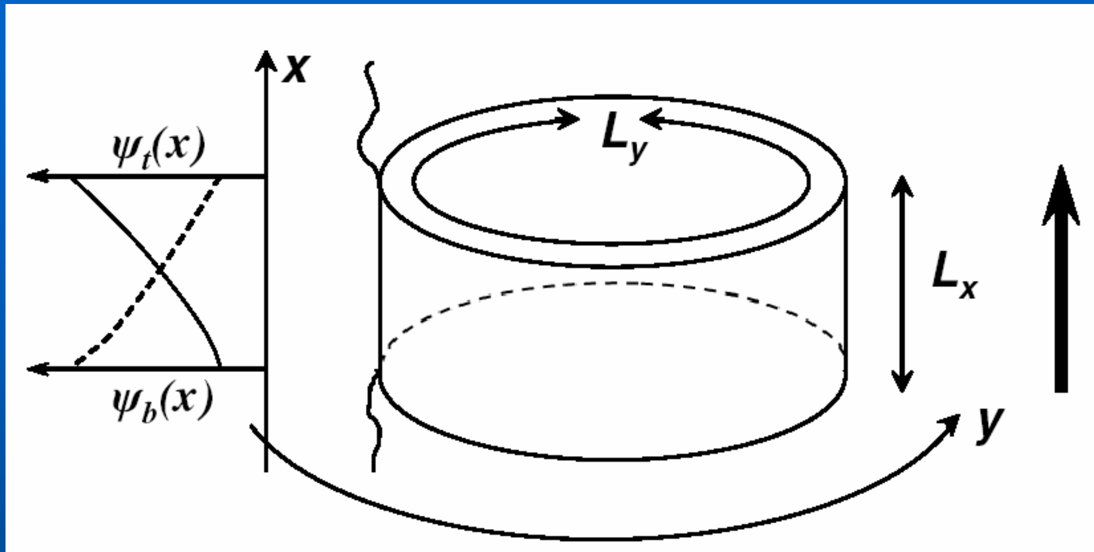

$$\psi_{\pm}(x, y) = \exp\left[\frac{2\pi n}{L_y}(x \pm iy)\right] \qquad n = 0, \pm 1, \pm 2, \ldots$$

$f(y+L_y) = f(y)$ Edge states near the top and bottom of the sample

New type of electron transport: via evanescent waves – different from both ballistic and diffusive

Transport via evanescent waves III

Leads from doped graphene

$$T_n = |t(k_y)|^2 = \frac{\cos^2\phi}{\cosh^2(k_y L_x) - \sin^2\phi}$$

$$\sin\phi = k_y / k_F$$

$$TrT = \sum_{n=-\infty}^{\infty} \frac{1}{\cosh^2(k_y L_x)} \simeq \frac{L_y}{\pi L_x}$$

Conductivity per channel: $e^2/(\pi h)$

The problem of “missing pi(e)” – may be, no problem

Other geometries by conformal mapping

(MIK and Guinea, PR B 2008; Rycerz, Recher and Wimmer, PR B 2010)

$$T_j = \frac{1}{\cosh^2[gj \ln \Lambda\{z(w)\}]}$$

$$j = \pm\frac{1}{2}, \pm\frac{3}{2}, \ldots$$

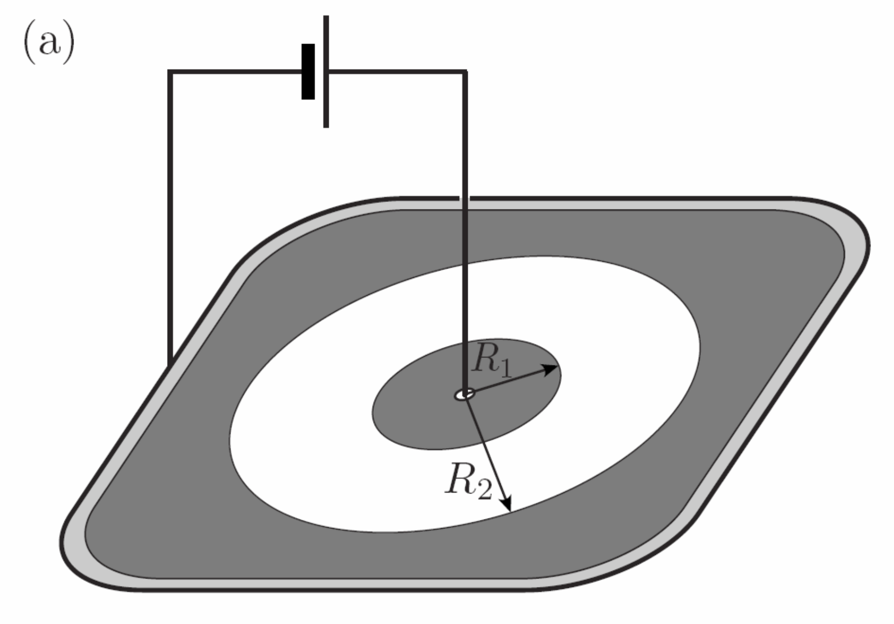

Λ transforms the region to circular ring (Corbino geometry)

$$G_{\mathrm{diff}} = \frac{2\pi\sigma_0}{\ln(R_2/R_1)}$$

Aharonov-Bohm effect at zero doping

MIK, EPL 89, 17001 (2009)

Magnetic flux tube within the ring

$$G = G_0 \left[1 - \frac{4\pi^2}{\ln\left(R_2/R_1\right)} \exp\left(-\frac{\pi^2}{\ln\left(R_2/R_1\right)} \right) \cos\left(\frac{e\Phi}{\hbar c} \right) \right]$$

General shape (topologically equivalent to rings)

$$G = G_0 \left[1 - \frac{4\pi^2}{\beta} \exp\left(-\pi^2/\beta \right) \cos\left(\frac{e\Phi}{\hbar c} \right) \right]$$

$$\beta = 2e^2/hG_0$$

$$\beta \ll \pi^2$$

Chiral tunneling and Klein paradox

MIK, Novoselov, Geim, Nat. Phys. 2, 620 (2006)

Electronics: heterostructures (*p*-*n*-*p* junctions etc.)

Classical particles: cannot propagate through potential barriers

Quantum particles: can propagate (tunneling) but probability decays exponentially with barrier height and width

Ultrarelativistic quantum particles: can propagate with the probability of order of unity (Klein paradox)

Klein paradox II

Ultrarelativisic

Nonrelativistic

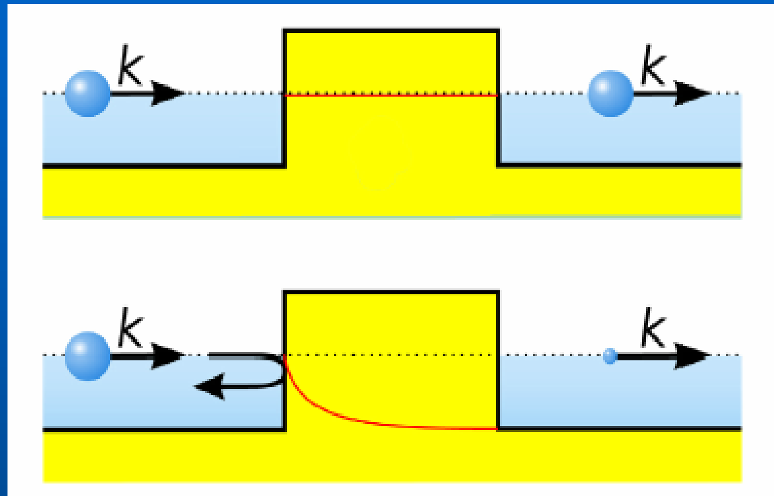

Tunnel effect: momentum and coordinate are complementary variables, kinetic and potential energy are not measurable simultaneously

Relativistic case: even the *coordinate itself* is not measurable, particle-antiparticle pair creation

Klein paradox III

Transmission probability

Barrier width 100 *nm*

Electron concentration
outside barrier 0.5×10^{12} cm^{-2}

Hole concentration
inside barrier 1×10^{12} cm^{-2}
(red) and 3×10^{12} cm^{-2} (blue)

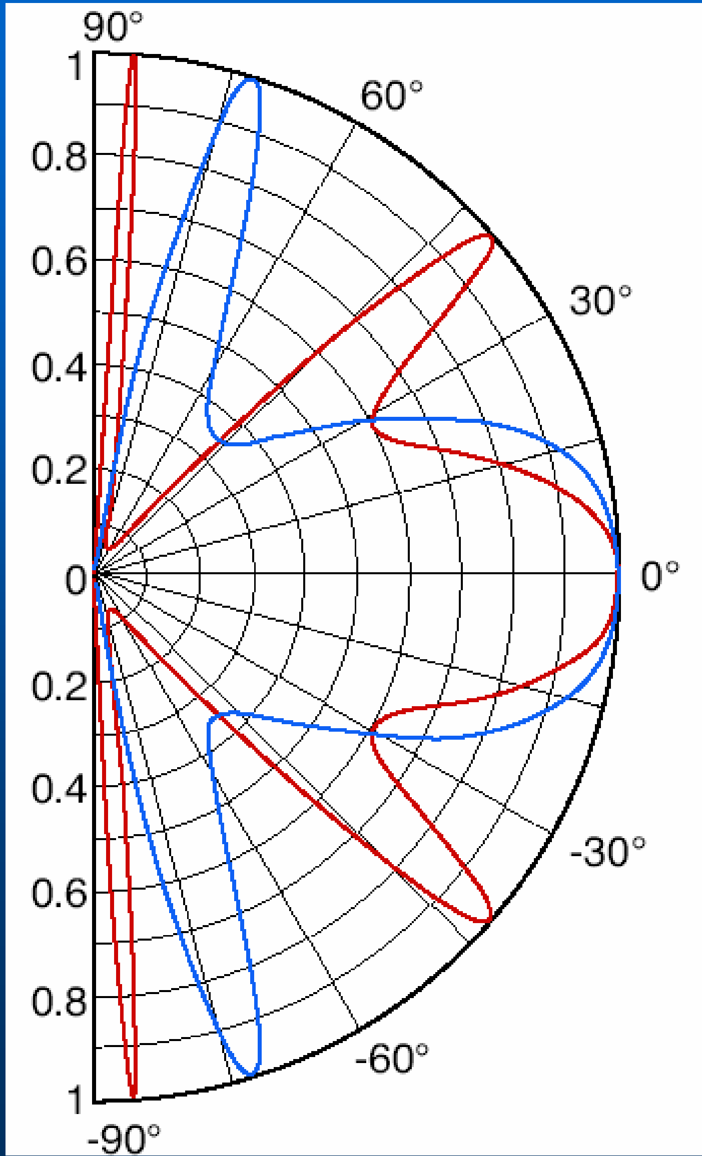

Klein paradox IV

Problem: graphene transistor can hardly be locked!

Possible solution: use bilayer graphene: chiral fermions with parabolic spectrum – no analogue in particle physics!

Transmission for bilayer; parameters are the same as for previous slide

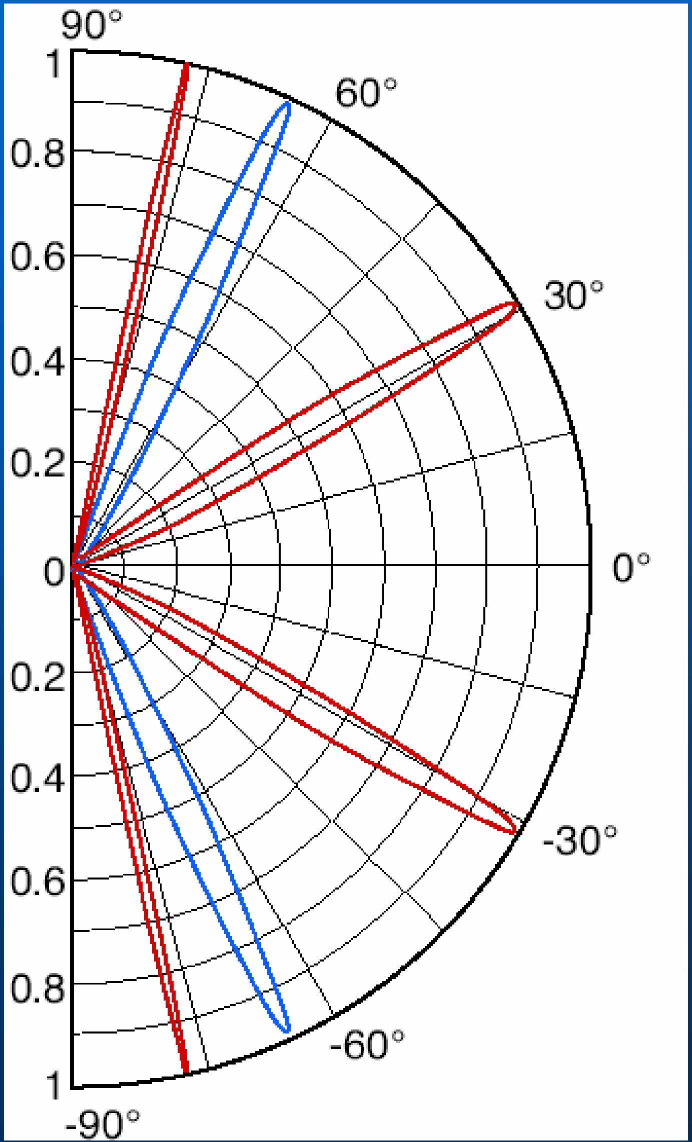

Semiclassical theory

T. Tudorovskiy, K. Reijnders & MIK, 2011

One-dimensional potential

$$\left[v\begin{pmatrix} 0 & \hat{p}_x - ip_y \\ \hat{p}_x + ip_y & 0 \end{pmatrix} + u(x/l) - E\right]\Psi = 0$$

$\tilde{x} = x/l$, $\tilde{p}_x = -ih\,d/d\tilde{x}$, $\tilde{p}_y = p_y/p_0$, $h = \hbar/p_0 l$, $\tilde{u} = u/vp_0$

$\widetilde{E} = E/vp_0$

Skipping tildas: the Hamiltonian

$$\hat{H} = \begin{pmatrix} 0 & \hat{p}_x - ip_y \\ \hat{p}_x + ip_y & 0 \end{pmatrix} + u(x)$$

Semiclassical theory II

Reduction to exact Schrödinger equations for complex potential

$$\left(\hat{p}_x^2 + p_y^2 - \nu(x)^2 - ih\sigma_x \nu'(x)\right)\Psi = 0$$

$$\nu(x) = u(x) - E$$

$$\Psi = \begin{pmatrix} 1 \\ 1 \end{pmatrix} \eta_1 + \begin{pmatrix} 1 \\ -1 \end{pmatrix} \eta_2$$

$$\left(h^2 \frac{d^2}{dx^2} + \nu(x)^2 - p_y^2 \pm ih\nu'(x)\right) \eta_{1,2} = 0$$

Canonical operator, expansion in *h* plus comparison with exact solution for linear potential (McCann & Falko, 2006)

Semiclassical theory III

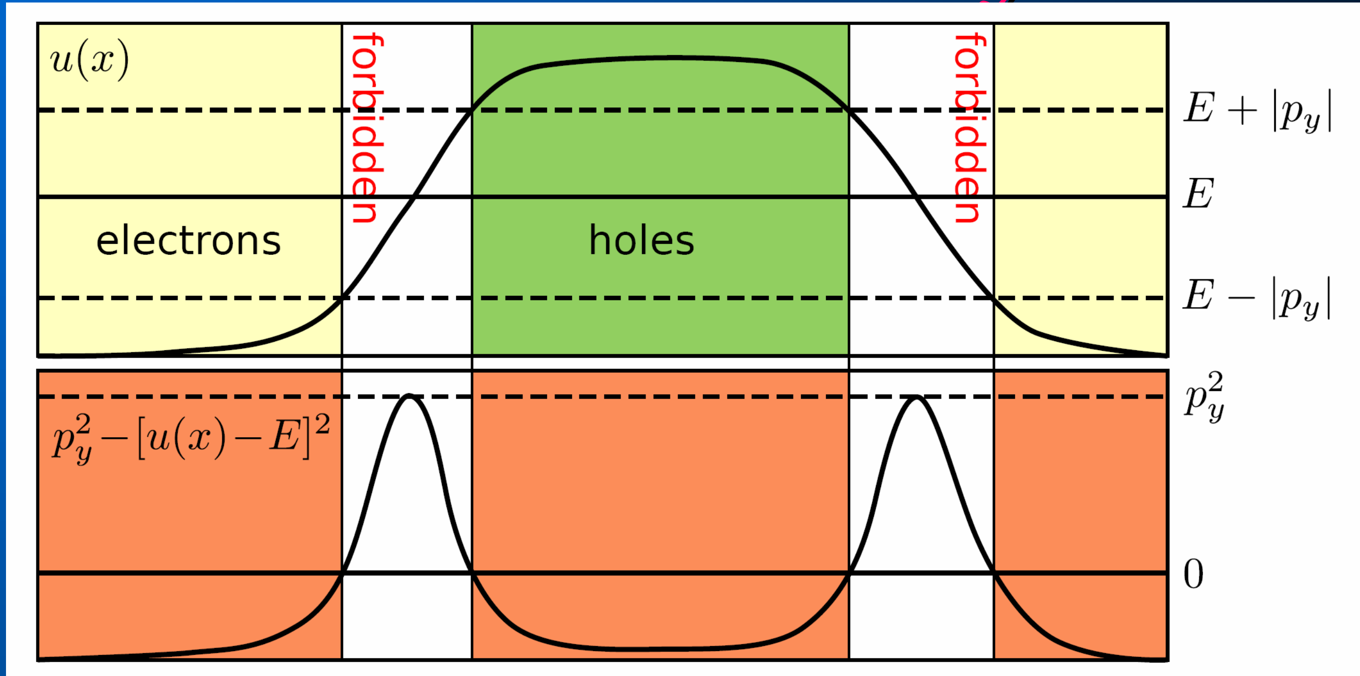

Fabry-Perot resonances

$$t_{res} \approx \frac{e^{-iL/h}}{\cosh(K_1/h - K_2/h)}$$

For nonsymmetric p-n-p junction 100% transmission – only at normal incidence

$$K_{pn} = \int_{x_1}^{x_2} dx' \sqrt{p_y^2 - v^2(x')}$$

Comparison with numerics

The angular dependence of the transmission coefficient for a particle of energy 80 meV incident on an n-p-n junction of height 200 meV. The barrier width $l_2 = 250$ nm and the n-p and p-n regions have characteristic lengths $l_1 = 150$ nm and $l_3 = 50$ nm, respectively. The blue line shows the numerical results for 99 steps, while the red line shows the uniform approximation (5.77).

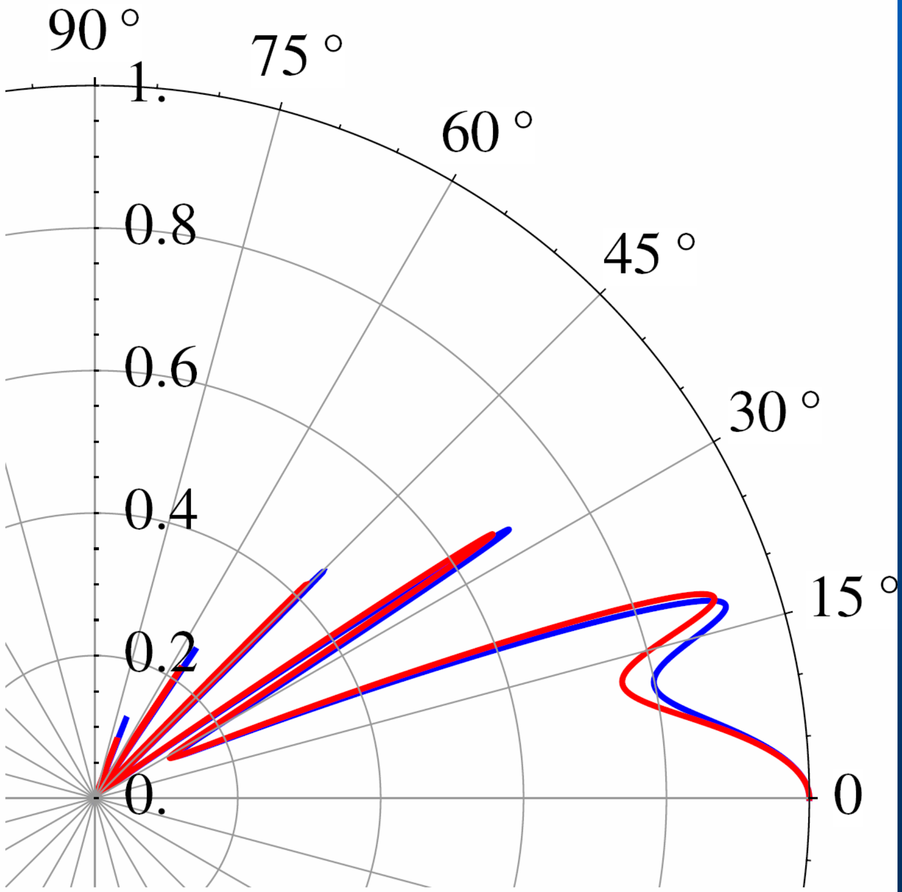

Asymmetric barriers

$$u(x/l_1) = \frac{U_{max}}{2}\left[1 + \tanh\left(10\frac{x}{l_1} - 5\right)\right]$$

Bilayer graphene

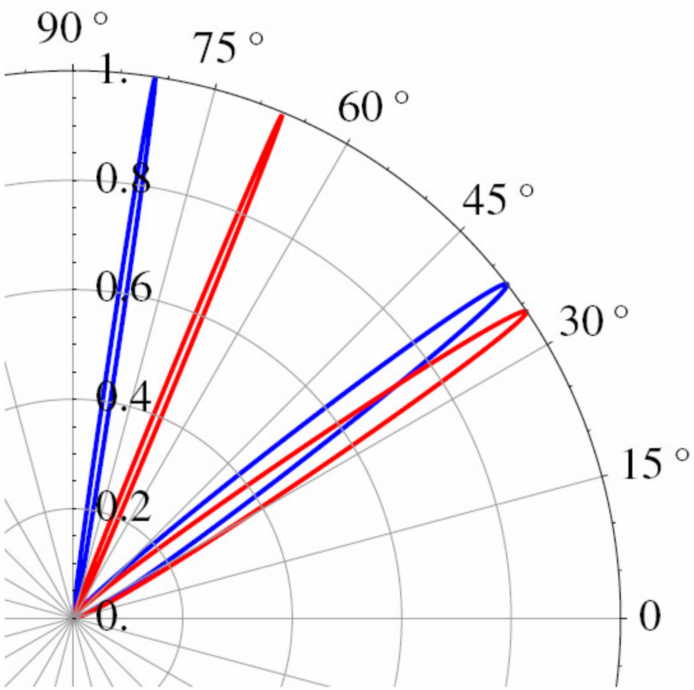

"Magic angles" with 100% transmission always exist (numerics)

Interesting and important theoretical problem (no obvious conservation law, etc.)

The angular dependence of the transmission coefficient for a particle of energy 17 meV incident on symmetric and asymmetric n-p-n junctions in bilayer graphene. Each junction has a height of 50 meV and a width $l_2 = 100$ nm. The blue line shows the numerical result for a symmetric junction with $l_1 = l_3 = 10$ nm, while the red line shows an asymmetric junction with $l_1 = 20$ nm and $l_3 = 40$ nm. All calculations were done with 99 steps per junction.

Klein tunneling: Experimental confirmation

PRL **102,** 026807 (2009) PHYSICAL REVIEW LETTERS week ending 16 JANUARY 2009

Evidence for Klein Tunneling in Graphene *p-n* Junctions

N. Stander, B. Huard, and D. Goldhaber-Gordon*
Department of Physics, Stanford University, Stanford, California 94305, USA
(Received 13 June 2008; published 16 January 2009)

Transport through potential barriers in graphene is investigated using a set of metallic gates capacitively coupled to graphene to modulate the potential landscape. When a gate-induced potential step is steep enough, disorder becomes less important and the resistance across the step is in quantitative agreement with predictions of Klein tunneling of Dirac fermions up to a small correction. We also perform magnetoresistance measurements at low magnetic fields and compare them to recent predictions.

nature physics LETTERS
PUBLISHED ONLINE: 1 FEBRUARY 2009 | DOI: 10.1038/NPHYS1198

Quantum interference and Klein tunnelling in graphene heterojunctions

Andrea F. Young and Philip Kim*

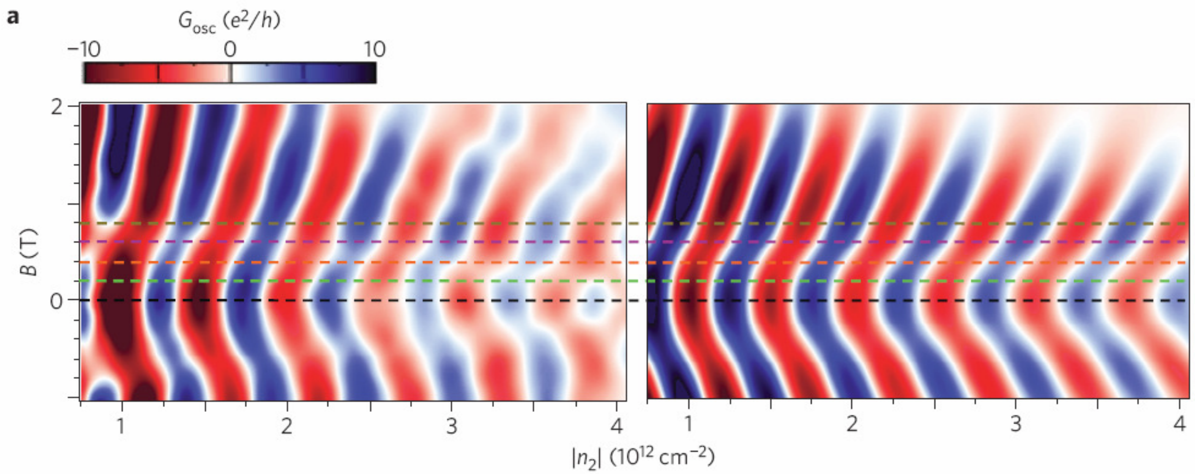

Klein tunneling prevents localization

Back scattering is forbidden for chiral fermions! Magic angle = 0
Nonuniversal magic angle for bilayer exists!

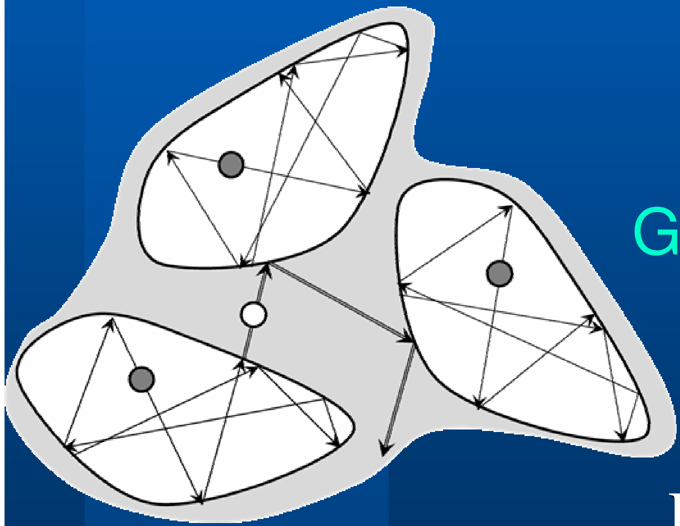

Graphene

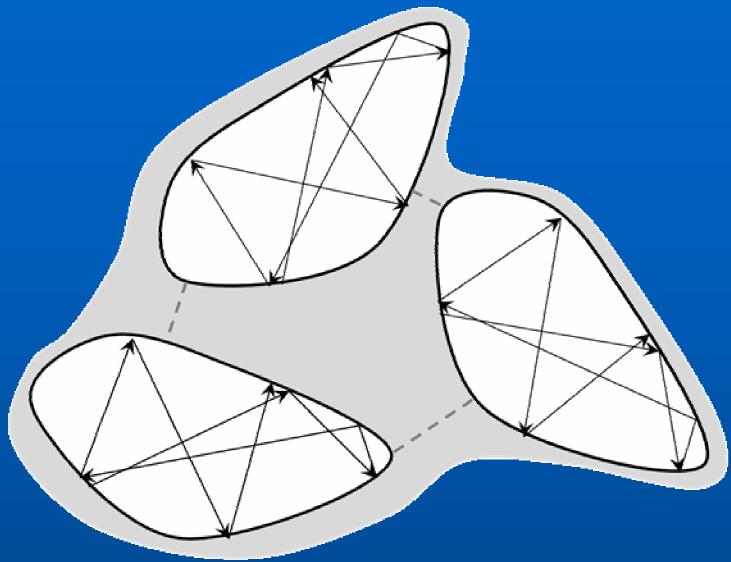

Conventional semiconductors

Electrons cannot be locked by random potential relief neither for single-layer nor for bilayer graphene – absence of localization and minimal conductivity?!

Quantum-Limited Resistivity

$$\sigma = ne\mu = \frac{e^2}{h} k_F l$$

Mott argument: $l \geq \lambda_F$

$$\sigma \geq \frac{e^2}{h}$$

(in the absence of localization)

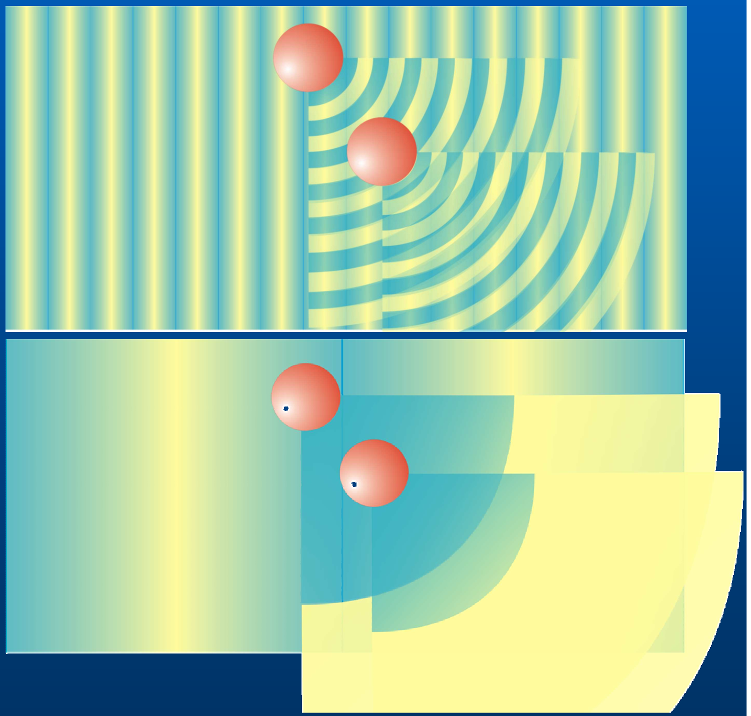

Inhomogeneities are unavoidable

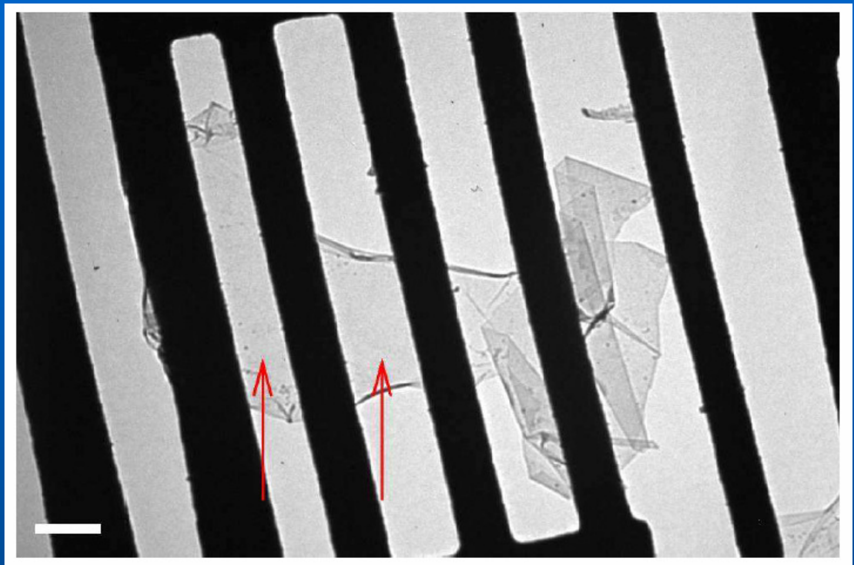

Freely suspended graphene membrane is corrugated

Meyer et al, *Nature 446, 60 (2007)*

2D crystals in 3D space cannot be flat, due to bending instability

Atomistic simulations of intrinsic ripples

Fasolino, Los & MIK, Nature Mater. 6, 858 (2007)

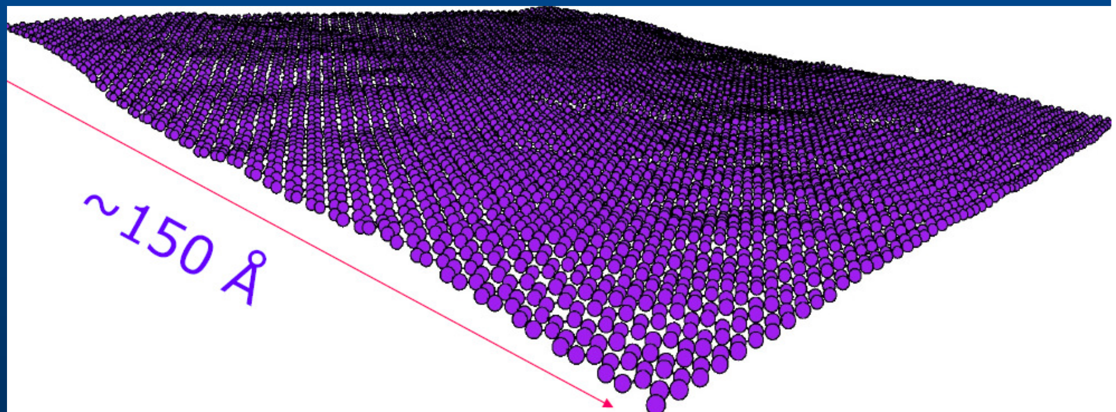

Chemical bonds

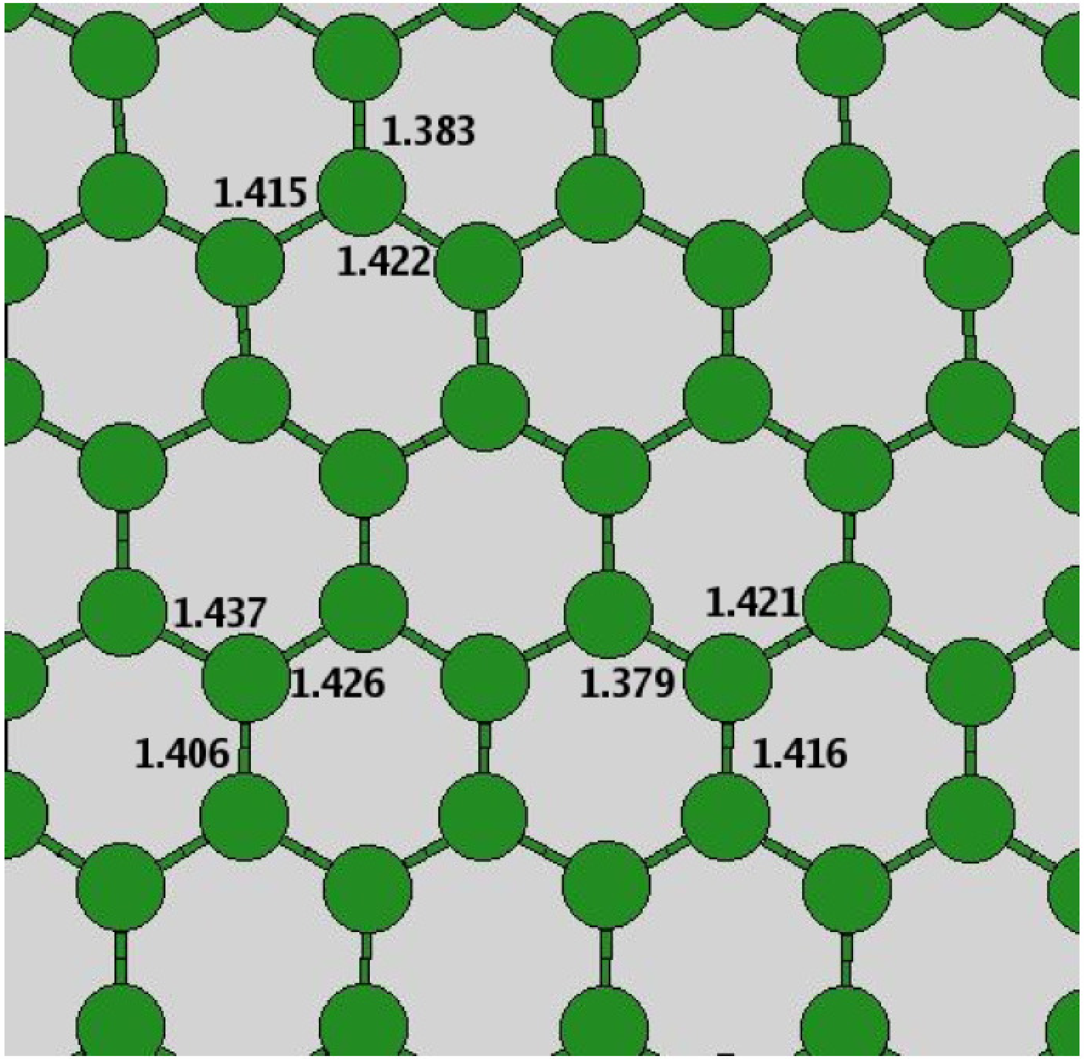

RT: tendency to formation of single and double bonds instead of equivalent conjugated bonds

Bending for "chemical" reasons

Pseudomagnetic fields

Nearest-neighbour approximation: changes of hopping integrals

$$\gamma = \gamma_0 + \left(\frac{\partial \gamma}{\partial \overline{u}_{ij}}\right)_0 \overline{u}_{ij}$$

$$H = v_F \sigma \left(-i\hbar\nabla - \frac{e}{c}\mathcal{A}\right)$$

"Vector potentials"

$$\mathcal{A}_x = \frac{c}{2ev_F}\left(\gamma_2 + \gamma_3 - 2\gamma_1\right),$$
$$\mathcal{A}_y = \frac{\sqrt{3}c}{2ev_F}\left(\gamma_3 - \gamma_2\right),$$

K **and** ***K'*** **points are shifted in opposite directions; Umklapp processes restore time-reversal symmetry**

Ripples and puddles

Gibertini, Tomadin, Polini, Fasolino & MIK, PR B 81, 125437 (2010)

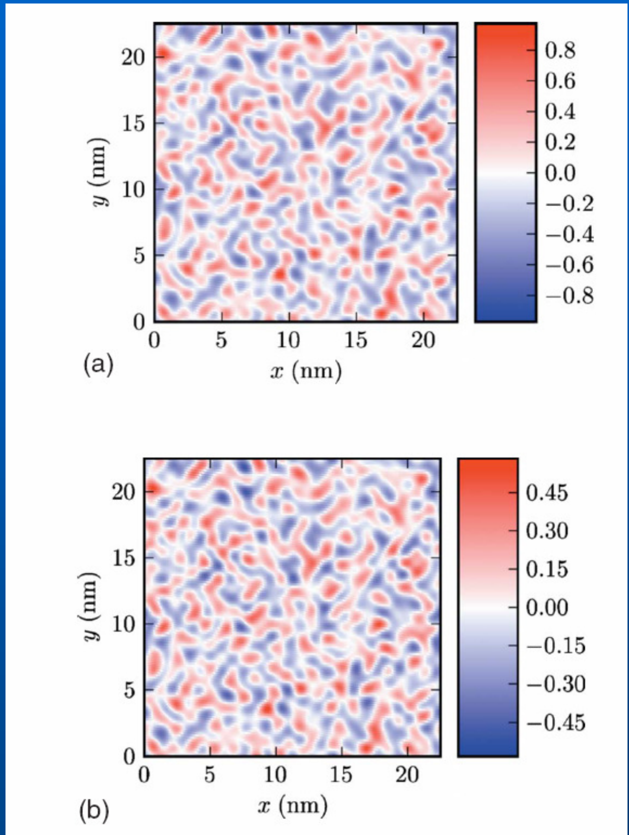

FIG. 4. (Color online) Top panel: fully self-consistent electronic density profile $\delta n(\boldsymbol{r})$ (in units of 10^{12} cm^{-2}) in a corrugated graphene sheet. The data reported in this figure have been obtained by setting $g_1=3$ eV, $\alpha_{ee}=0.9$ (this value of α_{ee} is the commonly used value for a graphene sheet on a SiO_2 substrate), and an average carrier density $\bar{n}_c \simeq 0.8\times10^{12}$ cm^{-2}. Bottom panel: same as in the top panel but for $\alpha_{ee}=2.2$ (this value of α_{ee} corresponds to suspended graphene).

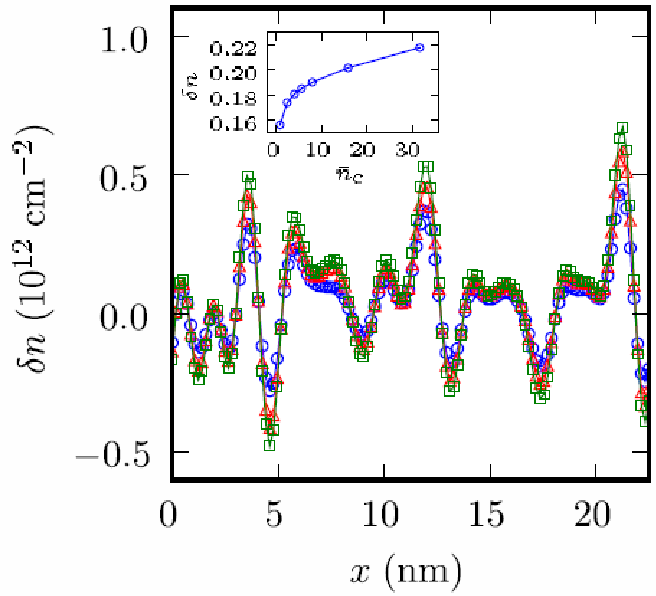

FIG. 9. (Color online) One-dimensional plots of the self-consistent density profiles (as functions of x in nm for $y=21.1$ nm) for different values of doping: $\bar{n}_c \simeq 0.8\times10^{12}$ cm^{-2} (circles), $\bar{n}_c \simeq 3.96\times10^{12}$ cm^{-2} (triangles), and $\bar{n}_c \simeq 3.17\times10^{13}$ cm^{-2} (squares). The data reported in this figure have been obtained by setting $g_1=3$ eV and $\alpha_{ee}=2.2$. The inset shows $\delta n(\boldsymbol{r})$ (in units of 10^{12} cm^{-2}) at a given point $\boldsymbol{r}$ in space as a function of the average carrier density $\bar{n}_c$ (in units of 10^{12} cm^{-2}).

Gauge fields from mechanics: back to Maxwell

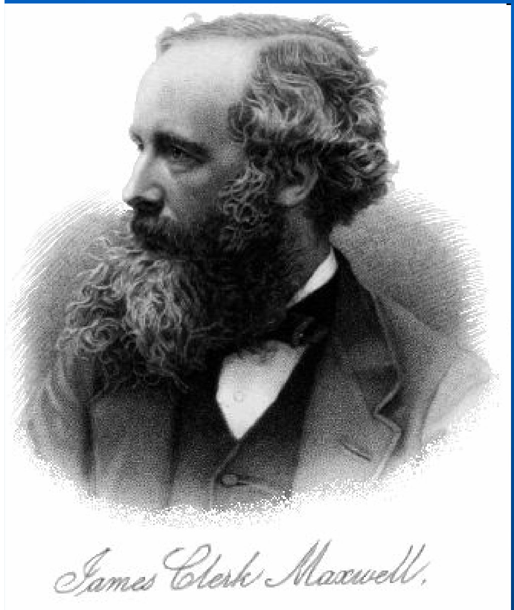

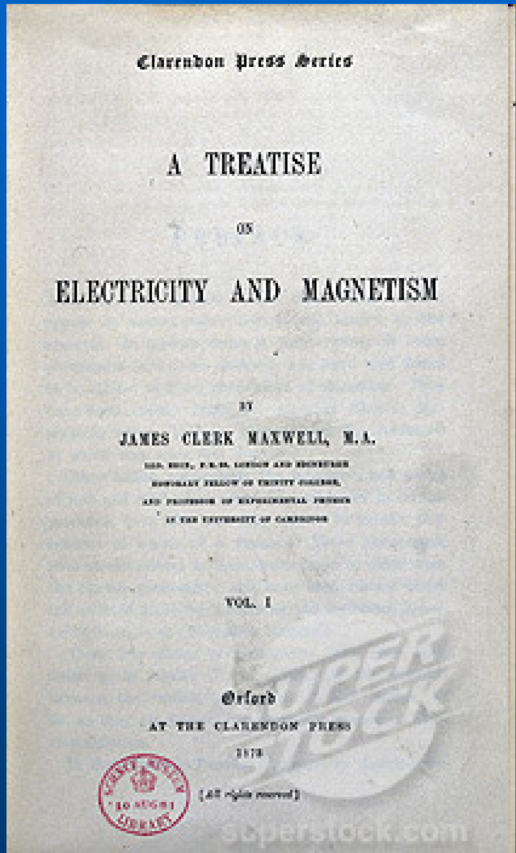

Clarendon Press Series

A TREATISE

ON

ELECTRICITY AND MAGNETISM

BY

JAMES CLERK MAXWELL, M.A.

VOL. I

Oxford

AT THE CLARENDON PRESS

[All rights reserved]

Electromagnetic fields as deformations in ether; gears and wheels

Review: Vozmediano, MIK & Guinea, Phys. Rep. 496, 109 (2010)

Zero-field QHE by strain engineering

F. Guinea, MIK & A. Geim, Nature Phys. 6, 30 (2010)

Within elasticity theory (continuum limit)

$$\mathbf{A} = \frac{\beta}{a}\begin{pmatrix} u_{xx} - u_{yy} \\ -2u_{xy} \end{pmatrix}$$

$$\beta = -\partial \ln t / \partial \ln a \approx 2$$

$$\begin{aligned} A_r &= \frac{\beta}{a}\left[\left(\frac{\partial u_r}{\partial r} - \frac{u_r}{r} - \frac{1}{r}\frac{\partial u_\theta}{\partial \theta}\right)\cos 3\theta \right. \\ &\quad \left. + \left(-\frac{1}{r}\frac{\partial u_r}{\partial \theta} + \frac{u_\theta}{r} - \frac{\partial u_\theta}{\partial r}\right)\sin 3\theta\right] \\ A_\theta &= \frac{\beta}{a}\left[\left(-\frac{\partial u_\theta}{\partial r} + \frac{u_\theta}{r} - \frac{1}{r}\frac{\partial u_r}{\partial \theta}\right)\cos 3\theta \right. \\ &\quad \left. + \left(\frac{1}{r}\frac{\partial u_\theta}{\partial \theta} + \frac{u_r}{r} - \frac{\partial u_r}{\partial r}\right)\sin 3\theta\right] \end{aligned}$$

Pseudomagnetic field

$$B_S = \frac{\partial A_y}{\partial x} - \frac{\partial A_x}{\partial y} = \frac{1}{r}\frac{\partial A_r}{\partial \theta} - \frac{\partial A_\theta}{\partial r} - \frac{A_\theta}{r}$$

Zero-field QHE by strain engineering II

Homegeneous magnetic field

$$u_r = cr^2 \sin 3\theta, \qquad u_\theta = cr^2 \cos 3\theta$$

$$B_S = 8\beta c / a$$

Three-fold symmetry

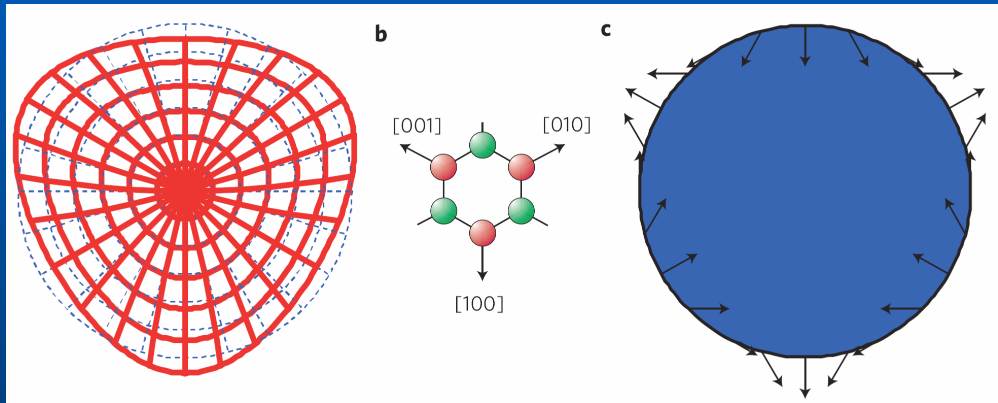

With normal forces only

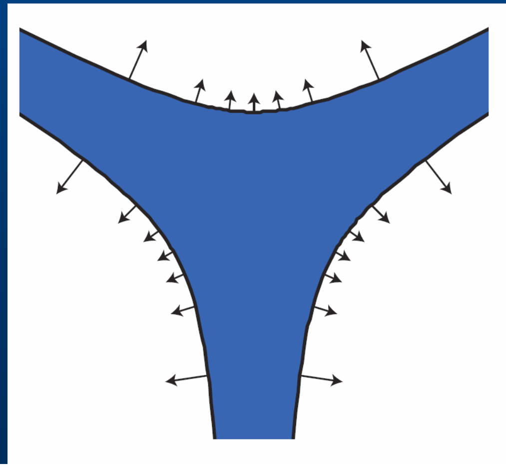

$$r(\theta) = \frac{const}{\left[(\cos\theta/2 \mp \sin\theta/2)(\pm 1 + 2\sin\theta)\right]^{2/3}}$$

Zero-field QHE by strain engineering III

Graphene: deformations up to 25%; at 10% pseudomagnetic fields of order 10-20 T. Can be a bit inhomogeneous

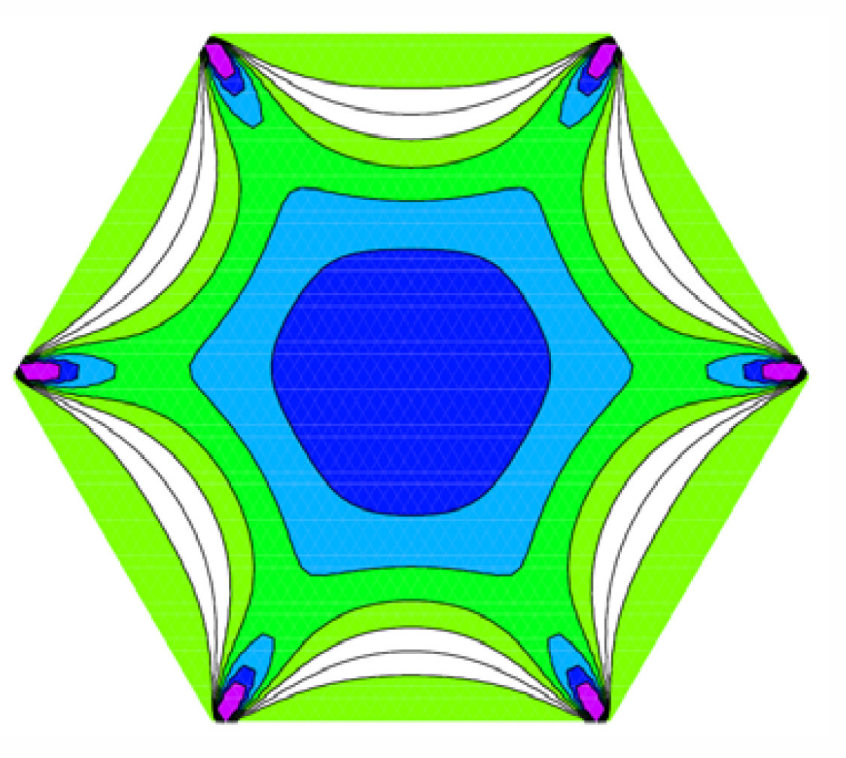

Normal stress applied to three edges, size 1.4 μm

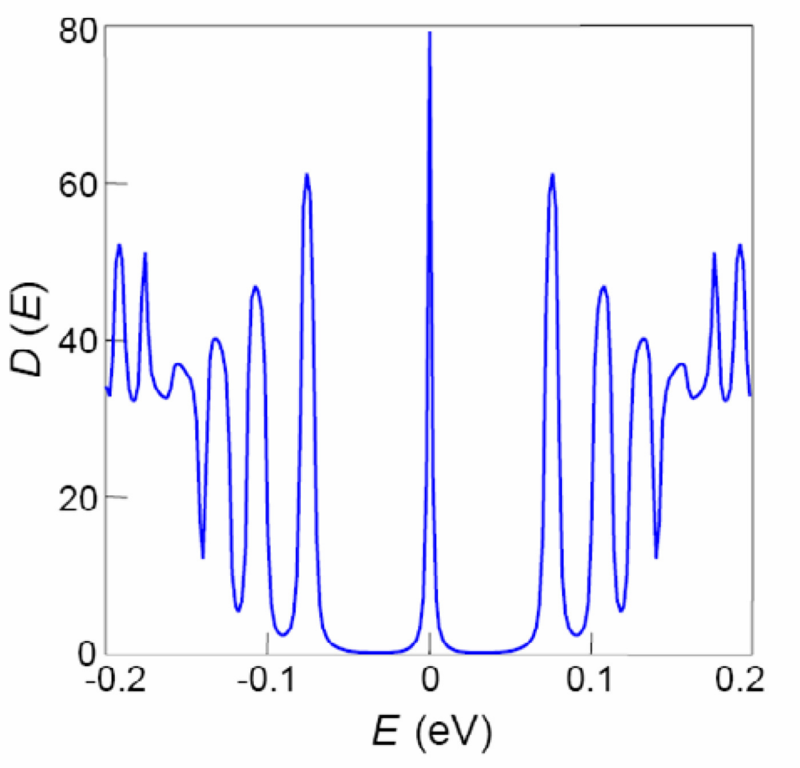

DOS in the center (0.5 μm)

Experimental confirmation?

Strain-Induced Pseudo–Magnetic Fields Greater Than 300 Tesla in Graphene Nanobubbles

30 JULY 2010 VOL 329 SCIENCE

N. Levy,[1,2]*† S. A. Burke,[1]*‡ K. L. Meaker,[1] M. Panlasigui,[1] A. Zettl,[1,2] F. Guinea,[3] A. H. Castro Neto,[4] M. F. Crommie[1,2]§

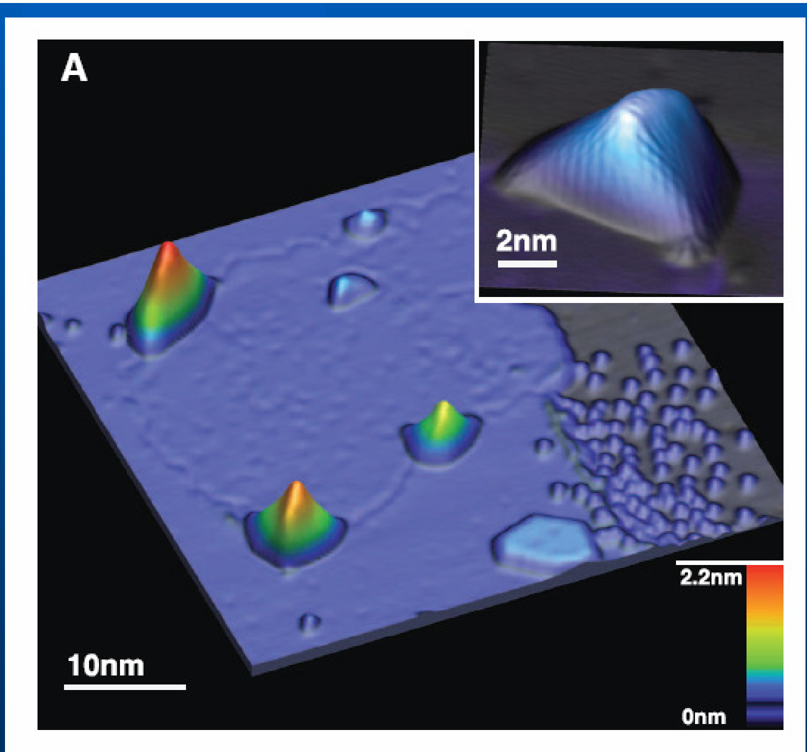

Graphene on Pt(111)

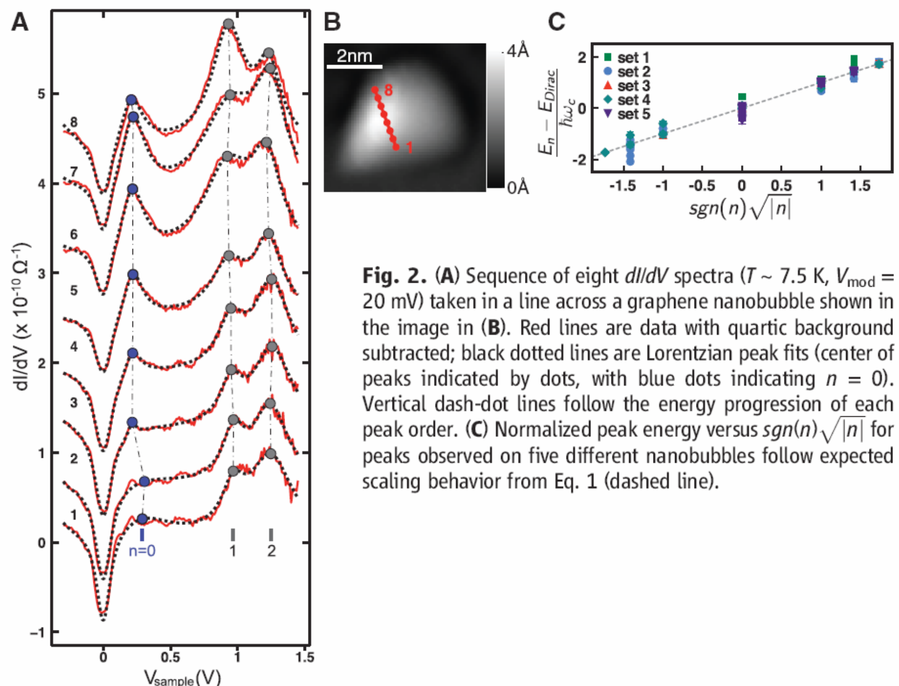

Fig. 2. (**A**) Sequence of eight *dI/dV* spectra ($T \sim 7.5$ K, V_{mod} = 20 mV) taken in a line across a graphene nanobubble shown in the image in (**B**). Red lines are data with quartic background subtracted; black dotted lines are Lorentzian peak fits (center of peaks indicated by dots, with blue dots indicating $n = 0$). Vertical dash-dot lines follow the energy progression of each peak order. (**C**) Normalized peak energy versus $sgn(n)\sqrt{|n|}$ for peaks observed on five different nanobubbles follow expected scaling behavior from Eq. 1 (dashed line).

STM observation of pseudo-Landau levels

Combination of strain and electric field: Haldane insulator state

(T. Low, F. Guinea & MIK, 2011)

Without inversion center combination of vector and scalar potential leads to gap opening

$$\Delta = -\mathrm{Tr}\left\{\sigma_z \frac{2}{v_F}\int d^2\vec{k}\,\frac{\mathrm{Im}\left(V_{-\vec{k}}\right)\left[(\vec{k}\vec{\sigma}),(\vec{A}_{\vec{k}}\vec{\sigma})\right]}{|\vec{k}|^2}\right\}$$

$$\propto \int d^2\vec{k}\,\frac{\mathrm{Im}(V_{-\vec{k}})\left(k_x A^y_{\vec{k}} - k_y A^x_{\vec{k}}\right)}{|\vec{k}|^2} \qquad (1)$$

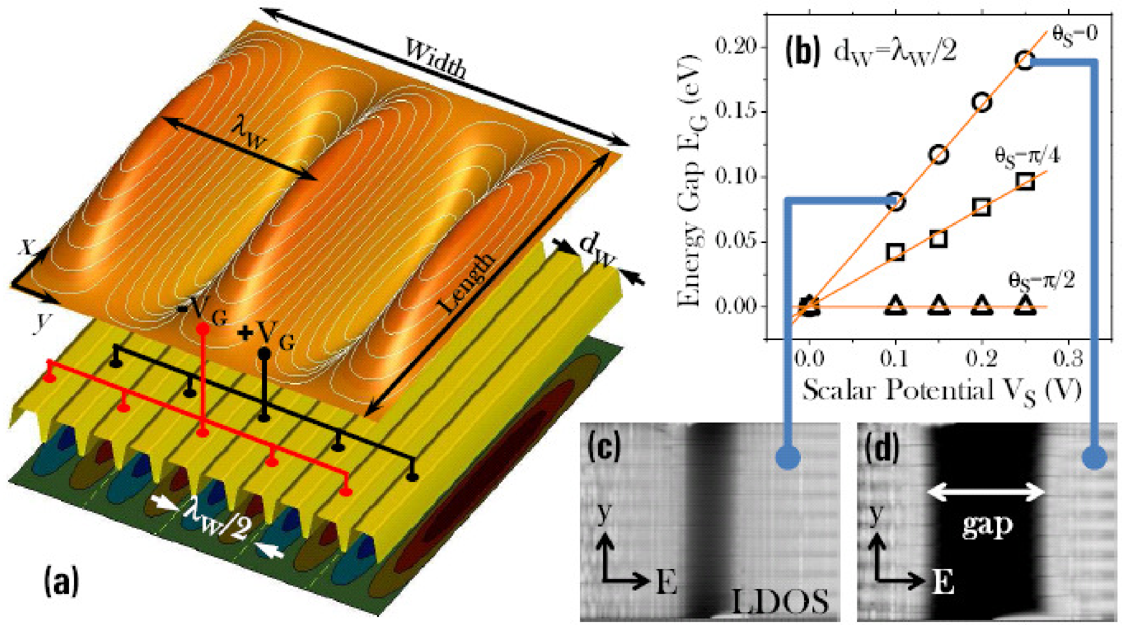

Wrinkles plus modulated scalar potential at different angles to the wrinkilng direction

Relativistic collapse for supercritical charges

Coulomb potential

$$V_0(\mathbf{r}) = \frac{Ze^2}{\epsilon r}$$

following Shytov, MIK & Levitov, PRL 99, 236801; 246803 (2007)

Naive arguments: Radius of atom *R*, momentum *ħ/R*. Nonrelativistic case:

E(R) ~ ħ² /mR² – Ze²/R

$E(R) \sim \hbar^2/mR^2 - Ze^2/R$

Minimum gives a size of atom.

Relativistic case: $E(R) \sim \hbar c^*/R - Ze^2/R$

Either no bound state or fall on the center.

Vacuum reconstruction at $Z > 170$

Supercritical charges II

Superheavy nuclei

I. Pomeranchuk and Y. Smorodinsky, J. Phys. USSR **9**, 97 (1945)

Graphene:
$v \approx c/300$,
$\alpha_{eff} \approx 1$

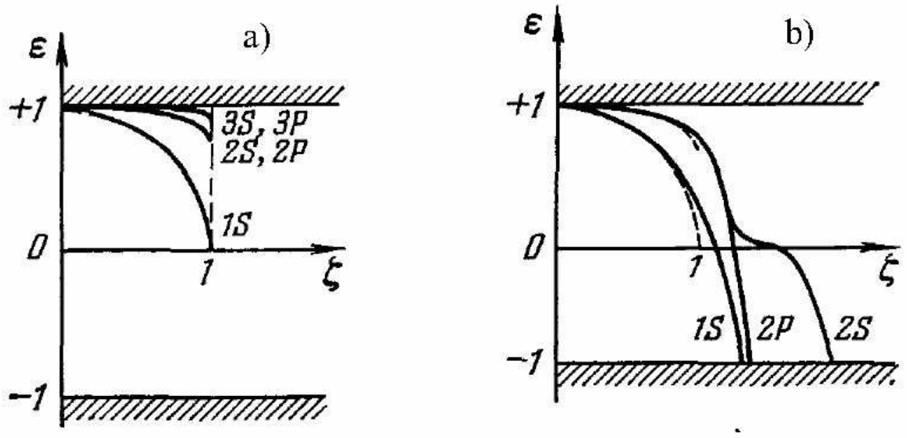

FIG. 1: a) Energy levels of superheavy atoms obtained from Dirac equation for Coulomb potential $-Ze^2/r$, plotted as a function of $\zeta = Z\alpha$, where Z is nuclear charge, and $\alpha = e^2/\hbar c$ is the fine structure constant. Energy is in the units of mc^2. (b) Energy levels for Coulomb potential regularized on the nuclear radius. As Z increases, the discrete levels approach the continuum of negative-energy states and dive into it one by one at supercritical $Z > 170$ (from Ref.[23]).

[23] Y. B. Zeldovich and V. S. Popov, Usp. Fiz. Nauk **105**, 403

Supercritical charges III

$\beta = Ze^2/\hbar v_F \varepsilon > 1/2$

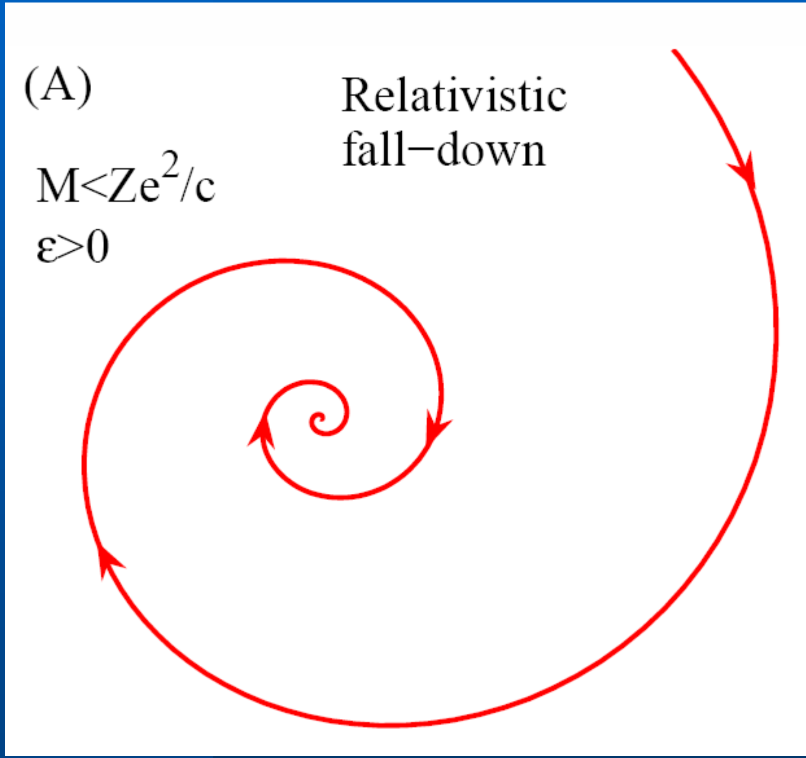

Quasi-local states

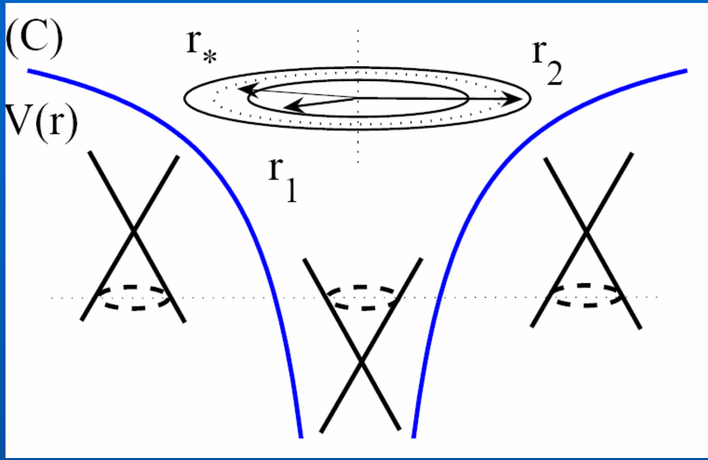

Klein tunneling

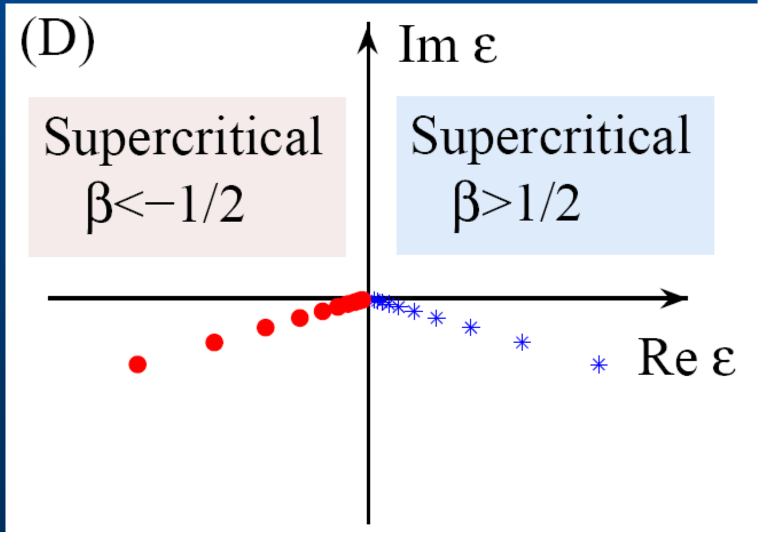

Supercritical charges IV

Interference of scattered wave and wave described electron fall to the centre leads to oscillations of electron density

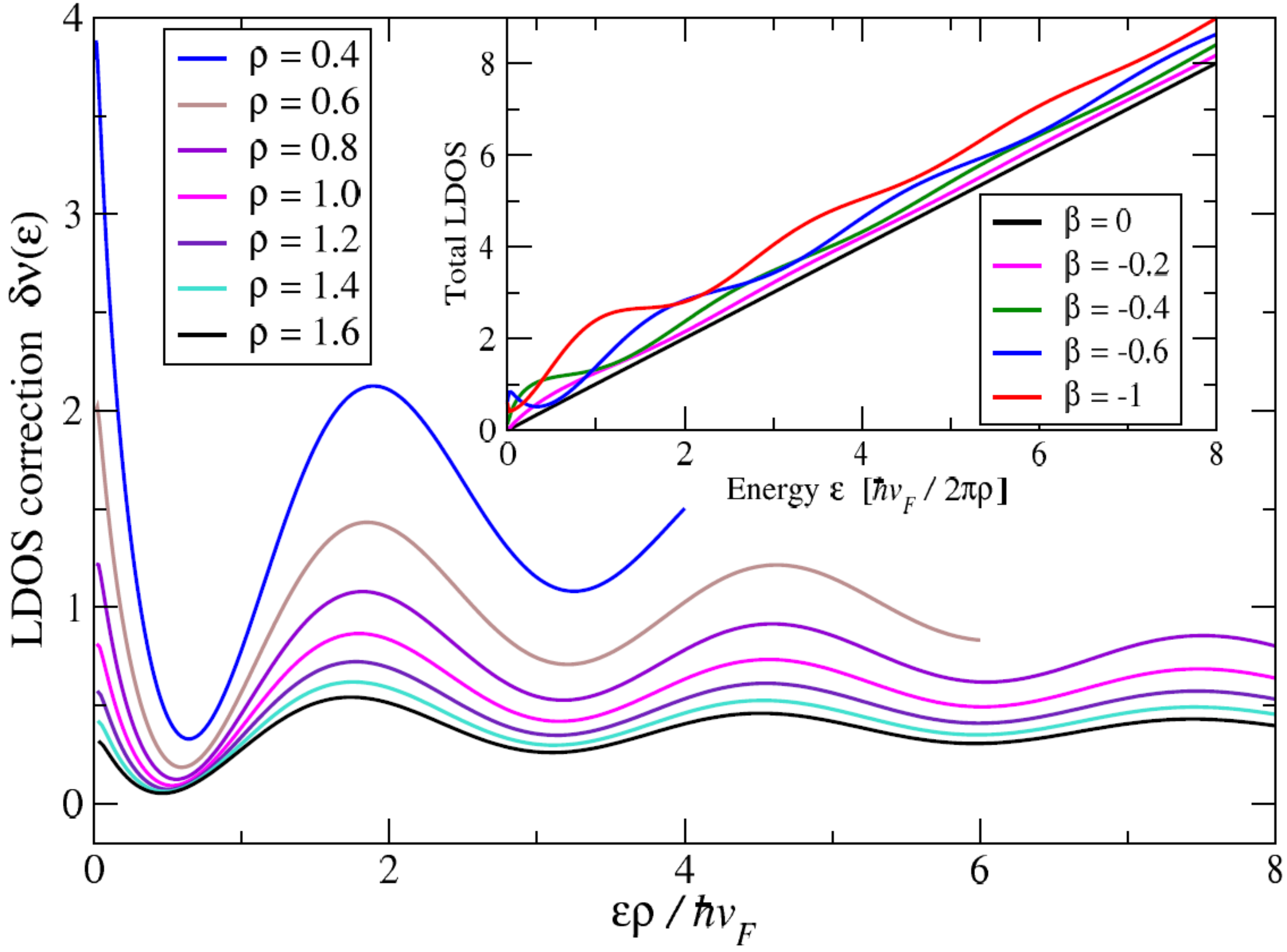

β = 0.6

Inset: oscillations for different charges

Supercritical charge V

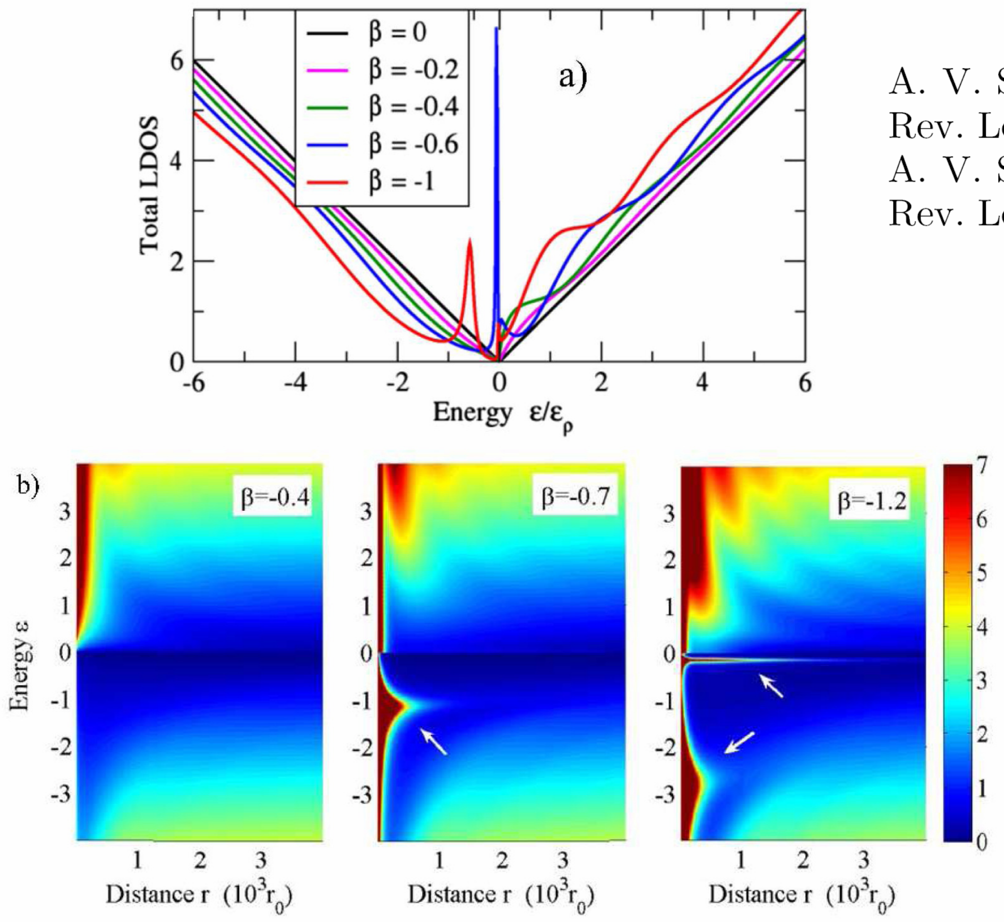

A. V. Shytov, M. I. Katsnelson, and L. S. Levitov, Phys. Rev. Lett. **99**, 236801 (2007), arXiv:0705.4663

A. V. Shytov, M. I. Katsnelson, and L. S. Levitov, Phys. Rev. Lett. **99**, 246802 (2007), arxiv.org:0708.0837

FIG. 3: (a) Local density of states (12) calculated at a fixed distance $\rho = 10^3 r_0$ from the charged impurity, where r_0 is a short-distance parameter of the order of carbon lattice spacing (from Ref.[10]). Peaks in the LDOS, which appear at supercritical β and move to more negative energies at increasing $|\beta|$, correspond to the resonant states. (b) Spatial map of the density of states, shown for several values of β, with resonances marked by white arrows (from Ref.[11]). Note that the spatial width of the resonances decreases at they move to lower energies, $\Delta\rho \propto 1/|\varepsilon|$, while the linewidth increases, $\gamma \propto |\varepsilon|$. The oscillatory structure at positive energies represents standing waves with maxima at $k\rho \approx (n + \frac{1}{2})\pi$, similar to those studied in carbon nanotubes [26]. Energy is given in the units of $\varepsilon_0 = 10^{-3}\hbar v/r_0 \approx 30\,\mathrm{mV}$ for $r_0 = 0.2\,\mathrm{nm}$.

Vacuum polarization effect and screening

Dimensional analysis: induced charge density in undoped graphene

$$n(r) = A\delta(\mathbf{r}) + B/r^2$$

If *B* is not zero: logarithmically divergent induces charge and “nullification” of Coulomb potential – predicted by Thomas –Fermi theory

MIK, PR B 74, 201401 (2006)

Linear screening theory: constant dielectric function, screening charge focused at the coordinate origin (only first term)

Screening II

$$n_{\mathrm{pol}}(\rho) = -\frac{N \,\mathrm{sign}\, \beta}{2\pi^2 \rho^2} \sum_{|m+\frac{1}{2}|<|\beta|} \sqrt{\beta^2 - \left(m + \tfrac{1}{2}\right)^2}$$

N = 4 (two valleys, two spins)

Large *β*: replacing the sum by an integral recover the Thomas-Fermi result

RG analysis: supercritical charge is screened to *β = ½* with a finite screening radius (similar to black hole horizon)

Conclusions and final remarks

- New type of transport in solids: quantum relativistic transport via evanscent waves
- Klein tunneling – a key phenomenon for graphene physics and applications
- Gauge fields are real mechanical fields, one can manipulate them
- Vacuum reconstruction? QED with strong interaction

Main collaborators

Andre Geim, Kostya Novoselov (Manchester)

Annalisa Fasolino, Jan Los, Kostya Zakharchenko, Rafa Roldan, Timur Tudorovskiy, Shengjun Yuan, Koen Reijnders (Nijmegen)

Leonya Levitov (MIT), Andrey Shytov (Exeter)

Paco Guinea, Maria Vozmediano (Madrid)

Marco Polini (Pisa), Misha Fogler (San Diego)

Tony Low (Purdue Univ.)